HHS Public Access

Author manuscript

Nat Genet. Author manuscript; available in PMC 2017 October 24.

Published in final edited form as:

Nat Genet. 2017 June ; 49(6): 876–886. doi:10.1038/ng.3848.

Stable Polycomb-dependent transgenerational inheritance of chromatin states in *Drosophila*

Filippo Ciabrelli[1], **Federico Comoglio**[2,3], **Simon Fellous**[4], **Boyan Bonev**[1], **Maria Ninova**[5], **Quentin Szabo**[1], **Anne Xuéreb**[4], **Christophe Klopp**[6], **Alexei Aravin**[5], **Renato Paro**[2,7], **Frédéric Bantignies**[1], and **Giacomo Cavalli**[1]

[1]Institute of Human Genetics, UMR 9002 of the CNRS and the University of Montpellier, 34396 Montpellier, France [2]Department of Biosystems Science and Engineering, ETH Zurich, 4058 Basel, Switzerland [4]CBGP-INRA, 755 Avenue du Campus Agropolis, CS30016, 34988 Montferrier sur Lez Cedex, France [5]Division of Biology, California Institute of Technology, Pasadena, California 91125, USA [6]Unité de Mathématiques et Informatique Appliquées de Toulouse, INRA, 31326 Castanet Tolosan, France [7]Faculty of Science, University of Basel, 4056 Basel, Switzerland

Abstract

Transgenerational Epigenetic Inheritance (TEI) studies the transmission of alternative functional states through multiple generations in the presence of the same genomic DNA sequence. Very little is known on the principles and the molecular mechanisms governing this type of inheritance. Here, by transiently enhancing 3D chromatin interactions, we established stable and isogenic *Drosophila* epilines that carry alternative epialleles, defined by differential levels of the Polycomb-dependent H3K27me3 mark. Once established, epialleles can be dominantly transmitted to naïve flies and induce paramutation. Importantly, epilines can be reset to a naïve state by disrupting chromatin

Correspondence should be addressed to: F.B. (frederic.bantignies@igh.cnrs.fr) or G.C. (giacomo.cavalli@igh.cnrs.fr).
[3]Current address: Cambridge Institute for Medical Research, Department of Haematology and Wellcome Trust/MRC Stem Cell Institute, Cambridge CB2 0XY, UK

URLs. BAM files containing uniquely aligned reads were pooled within each line using Picard http://picard.sourceforge.net. For DNA sequence analysis, the bcftools consensus methods described at https://github.com/samtools/bcftools/wiki/HOWTOs#consensus-calling.

Accession codes. gDNA-seq and RNA-seq data have been deposited in the Gene Expression Omnibus (GEO) and are available through accession GSE76799

Note: Any Supplementary Information and Source Data files are available in the online version of the paper

AUTHOR CONTRIBUTIONS

F.C. and G.C. initiated and led the project. F.C. designed and performed the experiments. F.C. and G.C. interpreted the data. F.C. and F.B. performed the FISH-I experiments. F.C., F.B. and Q.S. analyzed and interpreted the FISH-I experiments data. F.C. and F.B. performed the Antp[Ns] genetic crosses, scored the phenotypes and interpreted the data. F.C., S.F. and G.C. designed the experiments on environmental effects and interpreted the data. F.C., S.F. and A.X. performed the experiments on environmental effects. F. Comoglio analyzed genomic DNA sequencing data and performed bioinformatic analyses. C.K. analyzed sequencing data on the transgenic region. B.B. analyzed RNA-sequencing data and performed bioinformatic analyses. M.N. analyzed smallRNA-sequencing data and performed bioinformatic analyses. F.C., F.B., F.Comoglio, A.A., R.P., and G.C. composed the manuscript. All the authors reviewed and commented on the manuscript.

COMPETING FINANCIAL INTERESTS

The authors declare no competing financial interests.

interactions. Finally, we show that environmental changes can modulate the expressivity of the epialleles and we extend our paradigm to naturally occurring phenotypes. Our work sheds light on how nuclear organization and Polycomb group proteins contribute to epigenetically inheritable phenotypic variability.

In addition to DNA-encoded information, epigenetic mechanisms can potentially contribute to the transmission of heritable traits[1,2]. Transgenerational Epigenetic Inheritance (TEI) refers to such a transmisssion of information through multiple generations[3–5]. At the heart of TEI is the “epiallele”: the transgenerationally inheritable unit of epigenetic information. Epialleles might be induced for the same DNA sequence, either by environmental[6–9] or transient genetic perturbations[10–13]. Epialleles should be maintained in both soma and germline in subsequent generations. However, a molecular understanding of epiallele establishment, maintenance and erasure is still elusive and the very existence of epialleles remains contentious[3]. In a number of animal studies this type of inheritance was often weak and faded away within few generations[7,12,14]. Another common caveat of TEI studies is the lack of assessment for the potential contribution of cryptic genetic variation to the observed phenotypes, thus raising concerns on the *bona-fide* epigenetic nature of some of the described phenomena[3]. Three conditions are required to demonstrate TEI; i) the ability to carry out experiments in isogenic strains supported by a thorough verification of the genomic sequence; ii) the ability to revert epialleles into a naïve state at a frequency higher than expected by DNA mutation and iii) the identification of the epigenetic components at work.

Major regulators of gene expression as non-coding RNAs (ncRNAs)[6,13,15], cytosine methylation[8,10,11,16–18] and histone modifications[7,12] have been suggested to be linked to TEI. In *Drosophila melanogaster*, Polycomb Group Response Elements (PRE) are specific DNA sequences that can recruit Polycomb Group (PcG) and Trithorax Group (TrxG) proteins to chromatin[19]. Even if PcG proteins are known as major epigenetic players in the soma[20], little is known about their role in TEI. A PRE was previously shown to mediate TEI[21], but the robustness and stability of this effect as well as its molecular basis are not known. In order to explore the role of PcG proteins and of their nuclear organization[22–25] in TEI, we set out to generate stable *Drosophila* epilines upon a transient and reversible genetic perturbation. Our data identify a relationship between three-dimensional long-range chromatin interactions involving a PRE and the establishment, maintenance and erasure of epialleles. Alternative epialleles are characterized by developmentally persistent differential levels of the H3K27me3 mark and we identified a role for Polycomb Repressive Complex 2 (PRC2) in epiallele establishment and maintenance. We show that epialleles can be reset by impairing long-range chromatin interactions and we can exclude a contribution from DNA sequence variation. Furthermore, we identify a modulatory role for the environment on the expression and the short-term inheritance of epialleles, and we show that TEI can contribute to homeotic traits that do not depend on transgenes, suggesting that TEI can potentially contribute to phenotypic variation in natural *Drosophila* populations.

RESULTS

Establishment of stable epilines

As a paradigm for TEI in *D. melanogaster,* we employed PRE-containing transgenic lines. The Fab2L line carries a single-copy transgene inserted in chromosome arm 2L[26,27]. The 12.4 kb transgene contains the reporter genes *lacZ* and *mini-white* under the control of a 3.6 kb region called *Fab-7*, which contains a PRE and an insulator element[27,28]. The endogenous copy of the *Fab-7* region is located on chromosome arm 3R, where it controls the expression of *Abd-B,* a homeotic gene of the bithorax complex (Fig. 1a). The expression levels of *mini-white* determine the deposition of red pigment in the eyes, which display a typical PRE-dependent variegation[19,27] (Fig. 1a and Supplementary Fig. 1a,b). The eye phenotype is variable among individuals (Fig. 1a) and the degree of pigmentation depends on the opposing functions of TrxG and PcG proteins (Supplementary Fig. 1c). PcG-dependent repression at transgenes containing PREs can also be affected by the presence of the endogenous copy, even when located on a different chromosome[26]. This suggests that long-range chromatin interactions between the transgenic and the endogenous copies, which depend both on PcG proteins[26,29] and on insulator elements[30,31], modulate gene repressive and activating functions. In the Fab2L population, phenotypic differences among individuals correlate with expression levels of the *mini-white* and *lacZ* genes (Supplementary Fig. 1d) and differential deposition of the H3K27me3 mark at their Transcription Start Sites (TSS) (Supplementary Fig. 1e). However, these somatic epigenetic differences are not transgenerationally heritable, as self-crossing of flies with the most repressed or the most derepressed eye phenotypes for eight generations did not cause any phenotypic shift in the progenies (Supplementary Fig. 1f).

We thus decided to transiently perturb the interactions between the *Fab2L* transgene and the endogenous *Fab-7* locus, and test whether this might induce a transient plasticity in epigenetic states that could be conducive to TEI. To this aim, we first generated Fab2L flies carrying a heterozygous deletion of the endogenous *Fab-7* locus (F1 generation). We then self-crossed F1 flies to obtain F2 flies reconstituting the parental genotype (P0 Fab2L; +/+) (Fig. 1b). F2 flies with the least pigmented and the most pigmented eye colors were segregated in two distinct groups and self-crossed. The progenies of the two populations were subjected to selection based on the eye color for the following generations. Starting at the F3, we observed more pigmented flies in the selection of the active state and more reduced pigment levels in the selection of the repressed state. This trend further amplified across generations, with the first appearance of individuals in extreme phenotypic classes (i.e. totally red or totally white eyes) in the F5. The phenotypic differences among populations reached a plateau after ten and thirteen generations for the repressed and active state selections, respectively (Fig. 1b, right panel). Whereas the first line was hyperrepressed, with nearly complete white eyes, the other line appeared substantially derepressed, with every male exhibiting homogeneous red eyes at 21°C (Fig. 1c,d and Supplementary Fig. 2a). Even without selection after the F15, both lines stably maintained their different phenotypic trait over more than 50 generations (Fig. 1b). This scheme could be reproduced by introducing a different partial deletion in *Fab-7*, but not by any other mutation tested, including a deletion of the *Mcp* element, another regulatory region of *Abd-*

B containing a PRE and an insulator (Fig. 1b and Supplementary Fig. 2b). Moreover, selection of the derepressed phenotype could also be achieved starting from a different line called FabX[26,27] (Supplementary Fig. 3a,b), which carries a tandem insertion of a *Fab-7* transgene on chromosome X. Together, these results indicate that a transient loss of one copy of the endogenous *Fab-7* induces a plastic state in the F1, which allows the subsequent gradual establishment of exceptionally stable and phenotypically opposing fly lines.

To rule out a genetic contribution towards the observed phenotypes, we applied our selection scheme to Fab2L lines that had been previously isogenized in a Canton-S background. This led to a similar phenotypic segregation in these lines (Supplementary Fig. 4a,b), indicating that epilines can be established from congenic lines in a different genetic background.

Moreover, we deep sequenced the genomic DNA of the Fab2L line and the two newly generated lines in both Oregon-R and Canton-S genetic backgrounds at high coverage (>100x on average). In addition, we re-sequenced Oregon-R lines after eleven further generations. As typically observed in whole-genome sequencing of *Drosophila* isolates[31], SNP analysis identified hundreds of thousands of polymorphisms in each line (Fig. 1e). However, putative phenotype-associated SNPs, i.e. homozygous SNPs exclusively occurring in derepressed (Red*) or hyperrepressed (White*) in both genetic backgrounds and across generations were extremely limited in number (1 and 52 for Red* and White*, respectively) (Fig. 1e). No significant GO term enrichment was found for genes associated with SNPs (adjusted p-value < 0.05). Similarly, high-resolution analysis testing for 16 different types of structural variations (SVs) ranging from small insertions and deletions to complex chromosomal rearrangements[32] did not reveal line-specific signatures (Fig. 1e). Overall, only a handful of co-occurring SVs were annotated to coding sequences or gene promoters (Fig. 1e). None of these were associated to PcG/TrxG genes or to genes that could explain the observed eye pigmentation phenotypes (Supplementary Table 1). Furthermore, the transgenic *Fab-7, lacZ* and *mini-white* sequences were identical in each line, in both genetic backgrounds.

These results strongly argue against the possibility of selection of genetic variants during the establishment of the different lines, showing that their phenotypic differences are of epigenetic nature. Hereinafter, we will thus refer to the hyperrepressed and derepressed populations as Fab2L^{White*} and Fab2L^{Red*} epilines, respectively.

Epialleles transmit epigenetic information *in trans*

Next, we designed breeding schemes in order to determine the rules governing epiallele inheritance. Crossing Fab2L^{White*} or Fab2L^{Red*} epilines with Fab2L naïve flies revealed that the epialleles are pseudodominant over the naïve state, and epialleles are transmitted to the progeny more effectively from the mother than from the father (Fig. 2a and Supplementary Fig. 5a). To test whether the inherited epiallele is able to impose its epigenetic state to a naïve allele *in trans*, we recombined the naïve transgenic line with the *black[1]* recessive marker, which is only 6.4 cM away from the Fab2L insertion site. Homozygous *black[1]* induces a dark body pigmentation[33] (Supplementary Fig. 5b). Crossing Fab2L^{White*} or Fab2L^{Red*} with Fab2L, black[1] flies brings the epialleles in the presence of the naïve allele in the F1, and co-segregation of transgene and *black[1]* marker

allows to trace each allele across generations. Strikingly, the eye pigmentation level of homozygous *black[1]* F2 flies was undistinguishable from that of their siblings (Fig. 2b,c), thus indicating that the epiallele can transmit its epigenetic state *in trans* to the naïve allele. Moreover, once a naïve allele is converted into an epiallele in F2, it is able to transmit its state to another naïve allele, such that F4 flies carrying two copies of the latter show inheritance of the phenotype (Fig. 2b,c). When self-crossed, these flies can stably maintain the acquired epigenetic state at least until the F10 generation (Supplementary Fig. 5c). Therefore, epiallele inheritance displays a partial parent-of-origin effect and occurs by paramutation[34,35].

Epiallele induction and maintenance involve 3D chromatin interactions

Since physical contacts between PRE-containing sequences are mediated by long-range chromosomal interactions[29,36], we hypothesized that nuclear organization could play a role in establishment and/or maintenance of epilines. Thus, we measured the relative positioning of the transgenic and endogenous *Fab-7* loci by 3D Fluorescent in situ hybridization (3D-FISH). When compared to a w[1118] control, we found that the transgene locus was on average significantly closer to the endogenous *Fab-7* locus, both in the soma and in the germline (Supplementary Fig. 6a,b), and these long-range interactions were dependent on the presence of the endogenous *Fab-7* (Fig. 3a–d and Supplementary Fig. 7c,d). In F1 generation flies of the breeding scheme (Fig. 1b), i.e. Fab2L; Fab7[1]/+, which are hemizygous for the endogenous *Fab-7*, long-range interactions between the transgene and the endogenous *Fab-7* were significantly enhanced (Fig. 3a–d and Supplementary Fig. 6c,d). This correlates with unpairing of homologous copies of the endogenous locus, suggestive of competition between homologous and heterologous *Fab-7* copies for chromatin interactions (Supplementary Fig. 6e). These data suggest that, in the absence of a partner in the homologous locus in F1 generation Fab2L; Fab7[1]/+ embryos, the remaining endogenous *Fab-7* copy is less paired and can search more efficiently for transgenic copies. In order to find a mediator of this interaction, we measured the enrichment of GAGA factor (GAF), a known *Fab-7* binding protein that can facilitate chromatin interactions *in trans*[37]. Strikingly, not only GAF strongly binds to the insulator sequence of *Fab-7* in both Fab2L and in the two epilines, but its levels are significantly higher in Fab2L; Fab7[1]/+, in which the plastic epigenetic state is induced (Fig 3e). We then introduced a heterozygous null mutation of *Trl*, the gene encoding GAF, in Fab2L^{White*} and Fab2L^{Red*} epilines. The phenotypes of both epilines were partially suppressed (Fig. 3f,g), whereas other mutations in genes coding insulator proteins, such as *Cp190, su(Hw)* and *CTCF,* had no effect on epiallele maintenance (Figure 3f,g). These results suggest that GAF might be directly involved in the establishment and the maintenance of both epialleles by mediating 3D chromatin interactions.

FISH analysis shows that Fab2L^{White*} and Fab2L^{Red*} flies displayed shorter 3D distances between endogenous and transgenic loci compared to wt flies (Supplementary Fig. 7a–d). To test whether long-range chromatin interactions are involved in the maintenance of epialleles, we removed both copies of the endogenous *Fab-7* element from the epilines. Strikingly, this resulted in a complete reset of both silent and active epialleles (Fig. 4a). Of note, the presence of the endogenous copy of *Fab-7* - not a minimal number of *Fab-7* sequences in the genome - was necessary for epiallele maintenance (Supplementary Fig. 8a). Moreover,

deletion of the *Mcp* element had no impact on epiallele maintenance (Supplementary Fig. 8b). To further test the role of 3D interactions on epiallele maintenance, we changed the copy number of the transgene. Hemizygosity of the Fab2L transgene induces loss of chromatin contacts (Fig. 4b–e and Supplementary Fig. 9a,b). Consistent with the hypothesis that long-range chromatin interactions are required for the maintenance of epialleles, Fab2L^{White*} and Fab2L^{Red*} epilines crossed to wild-type (wt) w[1118] flies lead to F1 progenies with pale orange eyes (Fig. 4f). Therefore, both full repression and full activation depend on chromosome pairing, two phenomena known as pairing sensitive silencing[19] and pairing sensitive activation[38]. Self-crossing of F1 flies reestablished the Fab2L naïve phenotype in the F2 progeny carrying the homozygous transgene, regardless of the epigenetic state of Fab2L flies in the P0. This reset of chromatin states was robust, even upon further attempts to select hyperrepressed or derepressed eye phenotypes for up to 5 generations (Fig. 4f).

Altogether, these results suggest that the regulation of three-dimensional nuclear positioning is involved in the establishment and the maintenance of this TEI system. The inducible, specific and fully penetrant epiallele reversibility of the system further demonstrates its epigenetic nature.

PRC2-dependent histone modification marks epialleles in TEI

In order to generate epialleles, long-range chromatin contacts must ultimately trigger chromatin changes on the naïve *Fab-7* element in *cis. Fab-7* can recruit PcG and TrxG proteins[39], which determine a repressive and an active chromatin state, respectively. Consistent with a role for PcG function in silencing, we found a significant enrichment of the PRC2-dependent H3K27me3 mark on the transgene of adult Fab2L^{White*} flies, compared to Fab2L, which in turn exhibited higher H3K27me3 levels than in Fab2L^{Red*} (Fig. 5a). In contrast, the TrxG-associated H3K4me3 mark and H3/H4 acetylation marks were more enriched at the *lacZ* and *mini-white* promoters in Fab2L^{Red*} than in Fab2L^{White*} (Supplementary Fig. 10). In adult flies, these alternative chromatin states correlate with *lacZ* and *mini-white* mRNA levels (Fig. 5b).

Importantly, the transgene is not transcribed during embryogenesis (Fig. 5b), providing a window of opportunity to test whether chromatin marks predefine differential states before the onset of transcriptional differences. Although GAF is involved in the maintenance of epialleles, its level of binding in the epialleles is similar to that in their naïve counterpart (Fig. 3e–g), suggesting that *Fab2L^{White*}* and *Fab2L^{Red*}* might be marked by other chromatin components. Indeed, significant differences in H3K27me3 enrichment between Fab2L^{White*} and Fab2L^{Red*} epilines were detected in early embryos (Fig. 5a) and they even increased with progression to late embryogenesis (Supplementary Fig. 11a). At this stage, the transgenic locus was found to be associated more frequently to Polycomb foci (Supplementary 12a), displaying higher Polycomb signal intensities (Supplementary 12b) in Fab2L^{White*} compared to Fab2L^{Red*} flies. These data suggest that a perturbation of higher-order chromosome folding might underlie the ability of individual flies to gradually acquire a Polycomb hyperrepressed or derepressed epigenetic state. To test this hypothesis, we induced a transient heterozygous state for *E(z)*, the catalytic subunit of PRC2. We

hypothesized that a transient perturbation in PRC2 activity might induce a plastic state in the transgene that might allow subsequent epiallele selection. Since a defect in PRC2 function leads to loss of silencing, depletion of E(z) would be predicted to induce a derepressed epiline, whereas it should not generate a hyperrepressed one. After outcrossing the mutation to re-establish the wt Fab2L genotype, we applied the same selection scheme used to generate Fab2L^{White*} and Fab2L^{Red*} epilines. Consistent with the prediction, selection of red-eyed phenotypes led to a rapid, gradual establishment of a derepressed Fab2L line, similar to the Fab2L^{Red*} epiline (Fig. 5c,d), whereas no hyperrepressed line was obtained by selection of flies with lower eye pigmentation levels (Supplementary Fig. 13a). No stable derepressed epiline could be generated starting from Fab2L flies heterozygous for *Scm*, a PcG gene associated with PRC1 (Supplementary Fig. 13a), indicating that, although PRC1 is required for somatic gene silencing in the epilines (Supplementary Fig. 13b,c), its impaired function does not induce derepressed epilines (Supplementary Fig. 13a). These results are consistent with the activity of PRC2 and the absence of PRC1 function in the *Drosophila* germline[40].

We found no significant enrichments in embryos of the H3K4me3 mark (Supplementary Fig. 11b), nor for the other active marks tested (Supplementary Fig. 11c,d), suggesting that active chromatin marks might not underlie epiallele inheritance. This result was further supported by the inability of TrxG mutants to induce epialleles (Supplementary Fig. 13a), although TrxG members affect the somatic expression of the reporter genes, in both the naïve state (Supplementary Fig. 1c) and the Fab2L^{Red*} epiline (Supplementary Fig. 13c).

Transcription of non-coding RNAs (ncRNAs) at PREs has been shown to interfere with PRC2 activity in *Drosophila*[41]. Since the epilines exhibit increasingly different H3K27me3 deposition during development (Fig. 5a and Supplementary Fig. 11a), we assessed whether production of ncRNAs might correlate with differential H3K27me3 levels and with opposing epigenetic states. While the derepressed state correlates with the expression of a long-ncRNA produced by the *Fab-7* element (Supplementary Fig. 14a,b), no small-ncRNA could be detected in somatic tissues (Supplementary Fig. 15a,b). Importantly, no transgene expression or specific long-ncRNAs or small-ncRNAs could be detected in unfertilized eggs and in adult ovaries of the epilines (Supplemetary Fig 16a–c), suggesting that long-ncRNAs do not explain germline transmission of differential epialleles.

Together, these results show that perturbation of PRC2 activity plays a role in the establishment of the epialleles and a developmentally persistent difference in the PRC2-dependent H3K27me3 deposition delineates the heritable chromatin features of the epilines.

Environmental influence on TEI

To examine whether the environment could affect epiallele expressivity and inheritance, we exposed Fab2L epilines to a range of external stimuli. Varying protein and carbohydrate concentrations in the diet had no effect on eye phenotype (Supplementary Fig. 17). Likewise, epiallele inheritance was similar in the progenies of young and aged flies (Supplementary Fig. 18). Next, we investigated the stability of the epilines in ecologically relevant conditions by recreating a natural environment in microcosms. We found that epiallele inheritance was not erased by environmental variation. However, all three lines

gradually became more repressed (Fig. 6a). Moreover, we observed that epiallele inheritance follows the rules of paramutation, also under natural environmental conditions (Supplementary Fig. 19). We further investigated the influence of abiotic factor fluctuations on the fidelity of epiallele expression. Expression variability of the Fab2L^{Red*} epiallele was higher under variable hot conditions than in variable cold or stable conditions (Supplementary Fig. 20). To narrow down the effect of temperature on epiallele expression and inheritance, we exposed Fab2L, Fab2L^{White*} and Fab2L^{Red*} to a range of constant temperatures for two generations. Consistent with previous observations[27,42], high temperature exposure reduced pigmentation levels (Fig. 6b and Supplementary Fig 21a). To test whether this environmentally induced phenotypic change entails an irreversible epiallele erasure, we reared Fab2L^{Red*} flies at 28°C and 29°C for two generations, followed by 5 generations of self-crossing at 21°C, but no selection on eye phenotype. Strikingly, the progeny gradually regained the de-repressed state of their ancestor in 3 to 4 generations (Fig. 6c). Interestingly, the only developmental windows of temperature susceptibility are parental gametogenesis and embryogenesis (Supplementary Fig. 21b).

These results show the presence of an additional environmentally induced epivariable that acts upon the *Fab2L^{Red*}* epiallele and is reversible within few generations. This epigenotype-by-environment interaction is analogous to well-known genotype-by-environment interactions[43], and might add a layer of complexity in the appearance of phenotypes as a function of genetic and epigenetic makeups.

TEI of a homeotic trait

Finally, we tested whether epialleles could similarly be generated starting from lines carrying mutant alleles in a non-transgenic context. The *Nasobemia (Ns)* allele of the *Antennapedia* (*Antp*) gene is a spontaneous neomorphic mutation causing an antenna to leg homeotic transformation[44]. Previous work has shown that the *Antp* gene interacts in the three-dimensional nuclear space with the 10 Mb-distant *Fab-7* locus of the bithorax complex[29]. This long-range chromatin interaction can stabilize PcG-mediated silencing. Indeed, the Antp[Ns] transformation phenotype is exacerbated by the lack of the endogenous *Fab-7*[29]. We reproduced this genetic interaction using the *Fab7[1]* allele. In order to test whether the perturbation of chromatin contacts involving Hox loci might induce TEI, we recombined out the *Fab7[1]* allele starting from the Antp[Ns],Fab7[1]/+,+ line. To induce unique recombination events, we performed five independent single-fly crosses (Fig. 7a). Strikingly, an enhanced transformation phenotype persisted in the F2 generation. Moreover, enhanced transformation phenotypes were stably maintained in the following three generations (Fig. 7b,c). Similar results were obtained when the *Fab7[1]* allele was recombined out using Canton-S flies (Supplementary Fig. 22). This type of epiallele establishment, characterized by a rapid accumulation of the derepressed state only, is reminiscent of the FabX^{Red*} epiline generation (Supplementary Fig. 3).

In summary, a genetic interaction occurring in a previous generation can establish an epiallele that increases the severity of the Nasobemia phenotype and that can be stably inherited through generations. As a corollary, our data also show that gradual establishment

and sequence homology between distant loci are not a necessary prerequisite for the establishment of a *Fab-7*-dependent epiallele.

DISCUSSION

We demonstrate that upon transient increase in long-range chromatin interactions a plastic chromatin state can be induced, leading to the establishment of stable epilines with divergent phenotypes. The epigenetic nature of their inheritable phenotypes is proven by three facts i) Epilines can be established in an isogenized context; ii) Extensive analysis of DNA sequence excludes a genetic contribution both *in cis* and *in trans*; iii) As soon as long-range chromatin interactions are impaired, epilines revert into a naïve state within a single generation. While the three-dimensional architecture of the loci is involved in the establishment, maintenance and erasure of such inheritance, PRC2 function is responsible for the acquisition of a specific epigenetic state *in cis*. Indeed, once the long-range chromatin interactions are enhanced, the chromatin locus is prone to acquire an active or a silent state. The establishment of either epigenetic state is driven by phenotypic selection and proceeds gradually. These alternative states are marked by different levels of H3K37me3, which affect the expression of the surrounding genes and finally determine the observed phenotypes (Figure 8). The combined action of Polycomb-mediated repression and chromatin interactions has already been shown to be important for the regulation of certain loci in the somatic tissues. The presence of insulators, combined with the action of PcG and TrxG proteins, can drive long-range chromatin interactions and finally affect gene expression[26,29–31]. In the *Drosophila* female germline, PRC2 deposits H3K27me3 specifically in the future oocyte. Conversely, PRC1 components cannot be detected on chromatin at this stage and germline-specific mutations in PRC1 are fertile[40], in agreement with the absence of effect for the *Scm* mutation in TEI. It is not known yet to which extent H3K27me3 is intergenerationally inherited, on which loci it is deposited and what its function is. On the other hand, nuclear architecture in the *Drosophila* germline is still unexplored. In principle, the somatic cooperation between Polycomb-mediated repression and chromatin interactions might be extended to the germline and might play a role in the inheritance of epigenetic information. Our results suggest that their synergism could be crucial for the correct establishment of the chromatin landscape in the next generation, not only in transgenic context but also at endogenous genes. Consequently, a misregulation of this process might induce transgenerationally inheritable epigenetic phenotypes. It is noteworthy that, in addition to intrinsic regulation, the acquired epigenetic state is sensitive to environmental temperature conditions, suggesting that the interplay between environment and the epigenome is at least partially transmitted through subsequent generations.

In conclusion, our work demonstrates the existence of robust TEI in animals and shows that changes in chromosomal architecture can underlie this phenomenon. The robustness of TEI and its interaction with genetic and environmental factors suggests that this phenomenon may play an important role in heredity, and therefore in the evolution of animal species.

ONLINE METHODS

Fly Stocks and handling

Flies were raised in standard cornmeal yeast extract media. Standard temperature was 21°C, with the exception of P0 and F1 crosses in the experiments of Fab2L and FabX epiallele establishment and their relative controls (Figure 1b, Figure 5c,d, Supplementary Figure 2b, Supplementary Figure 3a, Supplementary Figure 4a and Supplementary Figure 13a), for which temperature was 18°C. In the experiments where temperature-specific effect were tested (Figure 6b,c and Supplementary Figure 21a,b), 18°C, 21°C, 25°C, 28°C or 29°C temperatures were applied throughout fly development (Figure 6b,c and Supplementary Figure 21a) or during specific developmental stages (Supplementary Figure 21b). Adult male flies were counted for phenotype scorings, with the exception of Figure 7b, Supplementary Figure 2a, Supplementary Figure 3a, Supplementary Fig. 4b right panel, Supplementary Figure 8a and Supplementary Figure 22, for which female flies were scored. The sample sizes were chosen according to common procedures in Drosophila genetics, maximizing statistical power compatibly with common practice in genetics labs. See the figure legends for more information on sample sizes. The Fab2L, Fab2L;Fab7[1], FabX;Fab2L;Fab7[1] lines were described in Bantignies et al., 2003[26]. Fab2L Canton-S and Fab2L;Fab7[1] Canton-S lines were generated from Fab2L and Fab2L;Fab7[1] lines. Those were backcrossed 7 times with w[1118] Canton-S flies, using single-fly crosses. Fab2L,black[1] were generated by recombining the Fab2L transgene with *black[1]* allele from the w[1118];black[1] line (Bloomington Drosophila Stock Center). Antp[Ns] and Antp[Ns];Fab7[1] were described in Bantignies et al., 2011[29]. The Oregon-R w[1118] line was used as wt control in the RT-qPCR, ChIP-qPCR and FISH assays. For pigmentation assay, the Oregon-R wt line was used as wt (wt) control. The other fly stocks were received from Bloomington Drosophila Stock Center.

Pigmentation assay

Thirty 4-days old adult male flies were decapitated by freezing in liquid nitrogen and subsequent vortexing. Heads were transferred into a collection tube and were homogenized with a micropestle in 20 µl EPE buffer (Ethanol 30% - HCl pH 2). After 1 hour at 25°C in the dark, the homogenized material was centrifuged twice at 12,000g for 3 minutes, supernatants were transferred to new tubes, and the absorbance at 480 nm O.D. of the final supernatants was measured against an EPE buffer blank. Absolute values were normalized to the wt control. Adult male fly heads were used for the assays, with the exception of the FabX cross in Supplementary Figure 3, in which adult female fly heads were used.

RT-qPCR assay

Thirty 4-days old adult male flies were decapitated by freezing in liquid nitrogen and subsequent vortexing. Heads were immediately frozen at −80°C; 4 to 8 hours old embryos and adult ovaries were collected in PBS buffer and immediately frozen at −80°C as pellet after washing. The biological samples were subsequently homogenized in 50 µl Trizol with a micropestle and the final volume was raised to 500 µl. After 5 minutes at room temperature, 100 µl chloroform was added to the samples, which were centrifuged at 12,000g for 15 minutes at 4°C. Total RNA was extracted with the RNA Clean & Concentrator kit (Zymo

Research) following manufacturer's instructions. RT was performed using 1 μg of total RNA with the Superscript III First Strand Synthesis Kit (Invitrogen), using hexamer primers and following manufacturer's instructions. cDNA quantifications were performed by real-time PCR (qPCR), using a Roche Light Cycler and the Light Cycler FastStart DNA Master SYBR green I kit. Expression levels were normalized to Act5C levels and adjusted accounting for the amplification efficiency of each oligo pair.

Chromatin immunoprecipitation and antibodies

Fifty 4-days old adult male flies were employed for histone ChIP, whereas two hundred 4 flies were employed for GAF ChIP. Flies were decapitated by freezing in liquid nitrogen and subsequent vortexing and heads were immediately frozen at −80°C; 4 to 8 hours old embryos and 8 to 12 hours old embryos were collected in PBS buffer and immediately frozen at −80°C as pellet after washing. Biological samples were crosslinked in 1 ml A1 buffer (60 mM KCl, 15 mM NaCl, 15 mM HEPES [pH 7.6], 4 mM MgCl2, 0.5% Triton X-100, 0.5 mM dithiothreitol (DTT), 10 mM sodium butyrate and complete EDTA-free protease inhibitor cocktail [Roche]), in the presence of 1.0% formaldehyde for histone modification ChIP and 1.8% formaldehyde for non-histone protein ChIP. Samples were homogenized with a micropestle and incubated for a total time of 15 minutes at room temperature. Crosslinking was stopped by adding 225 mM glycine followed by incubation for 5 min. The homogenate was transferred to a 1.5 ml tube and centrifuged for 5 minutes, 4,000g at 4°C. The supernatant was discarded, and the nuclear pellet was washed twice in 1 ml A1 buffer and once in 1 ml of A2 buffer (140 mM NaCl, 15 mM HEPES [pH 7.6], 1 mM EDTA, 0.5mM EGTA, 1%Triton X-100, 0.5mMDTT, 0.1% sodium deoxycholate, 10 mM sodium butyrate and complete EDTA-free protease inhibitor cocktail [Roche]) at 4°C. Nuclei were than resuspended in 100 μl A2 buffer in the presence of 1% SDS and 0.5% N-laurosylsarcosine and incubated for 30 minutes with agitation at 4°C. Chromatin was sonicated using a Bioruptor (Diagenode) for 16 min (settings 30 s on, 30 s off, high power). Sheared chromatin had size range of 300 to 700 base pairs. After sonication and 5 minutes high-speed centrifugation at 4°C, fragmented chromatin was recovered in the supernatant and the final volume was raised to 1 ml in A2 buffer with SDS 0.1%. Chromatin was precleared by addition of 50 μl of Protein A-Agarose (PA) suspension (Roche 11134515001) followed by overnight incubation at 4°C. PA was removed by centrifugation, antibodies at dilution 1:100 were added to the supernatant (a control in the presence of rabbit preserum [Mock IP] was performed at the same time), and samples were incubated for 4 hours at 4°C on a rotating wheel. PA (50 μl) was added, and incubation was continued overnight at 4°C. Antibody-protein complexes were collected by centrifugation at 350g for 1 minute, and supernatants were discarded. The supernatant of the mock IP was used as DNA Input control. Samples were washed four times in A3 (A2+ 0.05% SDS) buffer and twice in 1 mM EDTA, 10 mM Tris (pH 8) buffer (each 1ml wash lasted 5 minutes at 4°C on a rotating wheel). Chromatin was eluted from PA in 250 μl of 10 mM EDTA, 1% SDS, 50 mM Tris (pH 8) at 65°C for 15 minutes and eluted again in 250 μl of 10 mM EDTA, 0.67% SDS, 50 mM Tris (pH 8) at 65°C for 15 minutes, followed by centrifugation and recovery of the supernatant. The 500 μl eluates and the 1ml Input DNA samples were incubated overnight at 65°C to reverse crosslinks and treated with Proteinase K for 3 hours at 56°C. Sodium acetate (110 mM) was added to the samples, which were phenol-chloroform extracted and ethanol

precipitated in the presence of 20 μg glycogen. DNA was resuspended in 100 μl H_2O for IP samples and 500 μl H_2O for Input DNA samples. Immunoprecipitated DNA was used to analyze the enrichment of specific DNA fragments by real-time PCR (qPCR), using a Roche Light Cycler and the Light Cycler FastStart DNA Master SYBR green I kit. For each amplicon, IP DNA was normalized to Input DNA. The ChIP/Input ratio was further normalized to a negative control (RpL32, PGRP-LE or heterochromatic region). The ChIP amplicons, produced with the C,D,E,F,G,H oligo pairs, map to both transgenic and endogenous *Fab-7* regions. Antibodies used in this study were as follows: anti-GAF polyclonal antibody[45]; anti-H3K27me3 polyclonal antibody (Diagenode A1811-001P); anti-H3K4me3 monoclonal antibody (Millipore # 04-745); anti-H3K9/K14ac, polyclonal antibody (Sigma-Aldrich SAB4800007); anti-H4panacetylated polyclonal antibody (Millipore #06-598).

Two-color 3D FISH-Immunostaining protocol

Two-color 3D FISH-Immunostaining was performed as previously described[29]. For a detailed protocol, see Bantignies and Cavalli, 2014[46]. Briefly, embryos were dechorionated with bleach and fixed in buffer A (60 mM KCl; 15 mM NaCl; 0.5 mM spermidine; 0.15 mM spermine; 2 mM EDTA; 0.5 mM EGTA; 15 mM PIPES, pH 7.4) with 4% paraformaldehyde for 25 min in the presence of heptane. Embryos were then devitellinized by adding methanol to the heptane phase and sequentially re-hydrated in PBT (PBS, 0.1% Tween 20). Fixed embryos were treated with 100–200 μg/ml RNaseA in PBT for 2 hours at room temperature, and incubated in PBS-Tr (PBS, 0.3% Triton) for 1 hour. Embryos were then sequentially transferred into a pre-Hybridization Mixture (pHM: 50% formamide; 4XSSC; 100 mM NaH_2PO_4, pH 7.0; 0.1% Tween 20). Embryonic DNA was denatured in pHM at 80°C for 15 minutes. The pHM was removed, and denatured probes diluted in the FISH Hybridization Buffer (FHB: 10% dextransulfat; 50% deionized formamide; 2XSSC; 0.5 mg/ml Salmon Sperm DNA) were added to the tissues without prior cooling. Hybridization was performed at 37°C overnight with gentle agitation. Post-hybridization washes were performed, starting with 50% formamide, 2XSSC, 0.3% CHAPS and sequentially returning to PBT. Blocking was performed in PBS-Tr with 2% BSA for 2h and then, mouse primary anti-Aubergibne 4D10 (Siomi's laboratory), used at 1:1000 dilution or rabbit primary anti-Polycomb[29], used at 1:200 dilution, were incubated over night at 4°C. Embryos were washed in PBS-Tr and then an Alexa Fluor 647 conjugated secondary antibodies (Invitrogen life technologies) were added (1:500 dilution). After additional washes in PBS-Tr, DNA was counterstained with DAPI (at a final concentration of 0.1 ng/μl) in PBT and embryos were mounted with Vectashield (Clinisciences).

Probe Design and Labeling

For the *37B*/transgenic locus, we generated a 12 kb probe from 6 PCR fragments of 1.2 to 1.7 kb, which were spaced on average by 500 bp from each other, surrounding the 12.4 kb transgene region. For the *89E*/bithorax locus, we generated a 12 kb probe from 6 PCR fragments of 1.2 to 1.7 kb and spaced by 500 bp on average from each other, surrounding the 6kb endogenous *Fab-7* region. Oligo pair sequences for probe construction are listed in Supplementary Table 4. FISH Probes were generated using the FISH Tag DNA Kit with

Alexa Fluor 488 and 555 dyes (Invitrogen life technologies). Approximately 60 to 100 ng of each labeled probe diluted in 30 μl of FHB were used for hybridization.

Microscopy and Image Analysis

For the anti-Aubergine FISH-immuno, the 3D distances between *37B* and *89E* loci were acquired and measured as follows: due to somatic pairing of homologous chromosomes in *Drosophila*, the majority of the embryonic stage 14–15 nuclei in T1 and T2 show a single FISH spot for each probe. Conversely, most of embryonic stage 14–15 nuclei in the germline have unpaired homologous chromosomes. In the cases of non-overlap FISH signals between homologues, the closest distance between the centers of the two probes was considered. To measure distances, 3D stacks were collected from 3 different embryos at stage 14–15 in T1 and T2 embryonic segments and 6 different embryos at stage 14–15 in the germline, which are marked in their cytoplasm with the anti-Aubergine 4D10 antibody. Optical sections were collected at 0.5 μm intervals along Z-axis using a Leica SP8-UV microscope, Montpellier Rio Imaging (MRI) facility. Relative 3D distances between FISH signals were analyzed in approximately 100 to 120 nuclei per 3D stack in T1 and T2, and in approximately 10 to 12 nuclei per 3D stack in the germline, using the Metamorph software (Universal Imaging Corp.). The distance distribution between the two probes was obtained by pooling replicates for each condition. The classes were arbitrarily defined with a 500 nm range. In order to measure statistical significance between two distributions using a two-tailed Student's *t*-test, the normality of each distribution was assessed with Shapiro-Wilk test ($P>0.05$). To estimate the frequency of homologous unpairing, homologous loci were considered unpaired when the distance between the centers of their FISH spots was higher than 500nm. For the anti-Polycomb FISH-immuno, the colocalization levels between *37B* and Polycomb foci were acquired and measured as follows: 3D stacks were collected from 4 different embryos at stage 14–15 in T1 and T2 embryonic segments. Optical sections were collected at 0.3 μm intervals along Z-axis using the Leica SP8-UV microscope. Raw images from 3D stacks were deconvolved with Huygens Professional version 16.10 (Scientific Volume Imaging, The Netherlands), using the CMLE algorithm. After deconvolution, the FISH signals and Polycomb immunostaining were segmented in 3D using Imaris software (Bitplane, Switzerland). The centers of mass of the FISH signals were calculated and tested for their colocalization with the Polycomb segmented objects, using the XT module of Imaris. The intensity of the Polycomb staining in the centers of mass of Polycomb colocalized FISH objects was measured and normalized by the mean Polycomb intensity (measured in Polycomb segmented objects) for each stack. The percentage of colocalization and the normalized intensities were obtained by pooling replicates for each condition.

Genomic DNA sequencing

For each line, genomic DNA was extracted and purified from 150 adult female flies using the Gentra Puregene Cell Kit (Qiagen) following the manufacturer's instructions. Whole-genome overlapping paired-end (2x125 and 2x165 for Oregon-R and Canton-S flies, respectively) sequencing data were generated in three biological replicates. Library preparation and gDNA sequencing was performed by FASTERIS SA. Fastq files were aligned against the dm6 Drosophila reference genome using Bowtie2 v2.2.0[47] with standard parameters. Reads mapping to unplaced or unlocalized scaffolds were discarded, and BAM

files containing uniquely aligned reads were pooled within each line using Picard (see URLs section) and sorted and indexed using SAMtools v1.1[48]. SNPs were called using BCFtools v1.2. Line-specific SNPs were annotated with respect to genomic features and coding sequences using R 3.3.0/BioC and the VariantAnnotation package v1.18.7[49], and subjected to gene ontology analysis using Gorilla[50] with a p-value cutoff of 0.05. Structural variations (SVs) detection was carried out using the DSVD pipeline as previously described[32]. Seed-based alignment was performed using Bowtie2 v2.2.0 with parameters −3 95 –N 1 –L 30 –k 11. Sixteen different SV types, including small insertions and deletions, inversions and complex chromosomal rearrangements, were considered. Detected events were then filtered by discordant coverage, and SVs with a weight of 1 were discarded. All remaining line-specific high-confidence SVs were annotated to genomic compartments and coding sequences. Furthermore, we tested whether any mutation in the *Fab-7* region may be specific for any of the epilines. To this end, reads were aligned to the dm3 reference genome using bwa mem (v0.7.12-r1039). Alignment files were compressed, sorted and indexed with samtools v1.1. For each sample, a consensus sequence was called using vcf2fastq and the bcftools consensus methods (see URLs section). To verify the presence of the transgene, an in-depth profile of the *Fab-7* region with 2kb flanking regions was produced using samtools depth v1.1 and R. Variants within this region were called with the GATK haplotypeCaller v3.0.0 after removing PCR duplicates and recalibration. No epiline-specific variant was induced by the crossing scheme.

RNA sequencing

For each line, total RNA was prepared from adult heads or from unfertilized eggs as described in the RT-qPCR procedure. 4.5 μg of the material was sent for smallRNA sequencing and transcriptome sequencing to FASTERIS. Libraries for transcriptome sequencing were prepared after removal of rRNA (RiboZero step) and without PolyA purification step. Libraries for smallRNAs were prepared after removal of 2S RNA and polyacrylamide gel size selection of 18–30 nt. For the transcriptome sequencing, reads were mapped to the transgene sequence using STAR with default parameters and reads were visualized as reads per million (RPM). Data was visualized using the IGV browser[51]. Standard RNA sequencing data was mapped to the dm3 genome, the transgene sequence, and different *Fab-7* alleles, using two different approaches. First, full-length reads were mapped using bowtie2[47] with default parameters, which allows substitutions, insertion and deletions in the alignments. Second, reads were trimmed from their 3′-ends to 50 nt length and mapped with bowtie 0.12.7[52] allowing 0 mismatches and considering only uniquely mapping reads to the genome. Clean small RNA sequencing reads after Illumina adaptor clipping of sizes 15–44 nucleotides were mapped to the transgene sequence and different *Fab-7* alleles with bowtie2[47] with default parameters, and bowtie 0.12.7[52] allowing 0 or 3 mismatches. Small RNA mapping to the dm3 genome was performed with bowtie 0.12.7 allowing 0 mismatches and retaining uniquely mapping reads. Genome coverage tracks were generated using the bedtools suite[53], normalizing to the total number of mapped reads. For small RNA sequencing data, reads ranging between 20–29 nt length were further extracted and analyzed separately. Data was visualized using the IGV browser[51]. Read counts to different elements of the transgene were calculated using bedtools and a custom bash script. For gene expression analyzes, counts for uniquely mapping reads to a manually curated

annotations of protein-coding genes and non-coding RNAs obtained from RefSeq, miRbase, RFAM and Ensembl were calculated using a custom python script. Differential expression analyzes were performed using the DESeq2 R package[54]

Influence of the environment on epiallele expression and transmission

In Figure 6a and Supplementary Figures 17–20, we performed several experiments to investigate the influence of the environmental factors on epiallele expression and transmission. In Supplementary Figure 17, we reared flies in 10 different media varying in protein and digestible carbohydrate content. We varied carbohydrate/protein ratios and concentrations, spanning combinations of each nutrient from 12.5% to 200% of the standard composition of our nutritional medium, which is 26.3% for carbohydrates and 5.8% for proteins. Flies reared with the lowest concentration of proteins were not viable. In Supplementary Figure 18, we compared eye color in the progeny of either 5 or 40 days old parents. Three crosses were established per epiline and age treatment. In Figure 6a and Supplementary Figure 19, in order to investigate whether epiallele state is maintained and expressed in the fly's natural environment, we set up microcosms with natural plants and realistic abiotic conditions fluctuations. This was carried out at Ecotron Européen de Montpellier (CNRS) (www.ecotron.cnrs.fr). Three microcosms were set up per epiline. Flies were placed in 32cm*32cm*77cm cages with netting on the side and placed in chambers where temperature, humidity and light could be programmed to vary during the day. Programmed climate varied weekly, matching the weather observed in Montpellier, France, from April 7th to August 25th 2014 (see Supplementary Table 2 for programmed values). These cages contained an organic raspberry plant in a pot with live soil. Once a week, fly populations receive 2 cups with 20g of organic raspberries, sprayed with 5% nipagin and placed on a bed of wet soil. Cups were removed after 4–6 weeks, when we were certain no adult would emerge from them. Cups and plants were watered thrice weekly so as to avoid fruit and soil desiccation. After 3 months, plants started producing fruits on which the flies fed and reproduced. Numerous species were present in the cages: soil contained micro-arthropods (e.g. collembola), Sciaridae flies and earthworms; some plants were attacked by *Tetranychus urticae* spider mites that we actively controlled by releasing predatory *Phytoseilus sp* mites; one cage also saw the outbreak of predatory centipeds that caused the extinction of its Fab2L^{White*} population. As a result, the conditions experienced by the flies were markedly different from those in the laboratory. Population density varied from a dozen adults to thousands. Larvae developed in rooting fruits and pupated in the soil. Adult fly size varied accordingly, mirroring the harsh environment epilines developed in. Eye color was assayed three times during the course of the experiment by placing cups with raspberries and soil for 2 days in the cages, closing them with netting and phenotyping the emerging adults. This microcosm experiment was repeated with crosses between Fab2L^{Red*} and Fab2L,black[1] in three independent cages. The eye phenotypes and the body color were consequently scored. In Supplementary Figure 20, in order to disentangle the influence of biotic and abiotic conditions on epiallele dynamics, we performed an experiment in standard laboratory conditions but with three different treatments of temperature, light and humidity. The first one mimicked laboratory conditions with a constant temperature of 21°C and a fixed humidity level of 70%. The two other treatments corresponded to weather conditions observed in 5–11 June and 13–19 October 2013 in Montpellier, France (see Supplementary

Table 3 for programmed values). In the first one, temperature varied between 17.6°C and 26°C (mean 17.6°C), and between 13.7°C and 24°C in the second (mean 21.1°C). Temperature and relative humidity values represent the average of the 7 days for each of the time windows in the indicated weeks. The program was repeated for 12 weeks. There were 5 replicate bottles per epiline, which were flipped to new bottles every generation as is standard with fly cultures. At every generation, flies were scored for the eye phenotype and flipped in a new bottle All flies hence had similar ages and densities in the different treatments. The experiment lasted for 4 generations in the “17.6°C variable” treatment and 5 generations in the “21.1°C variable” and “21°C constant” treatments. During the experiment, a randomization was applied to cage positions within microcosms or incubators in order to avoid incubator-specific effects.

Antennapedia Nasobemia crosses

After population crosses in the P0, the TM3 balancer was outcrossed. Then, 5 single-fly crosses were performed in the F1. The idea behind single-fly crosses was to select flies deriving each time from a single recombination event. In the F2, wt flies for *Fab7* were selected. Then, at each generation, n<10 flies were selected to be crossed, regardless of the expressivity of the transformation phenotype. In the control cross on the right, flies were crossed with population crosses. After the outcross of the TM3 balancer in P0, the *Nasobemia* allele was positively selected in the following generations. Phenotypes were scored in a blinded fashion, *i.e.* by a researcher who had no knowledge of the identity of test and control crosses. Female adult flies were used for phenotype scorings. For electron microscopy (EM), adult female flies were coated with an approximate 10 μm thick gold film and then examined under a scanning EM (Hitachi S4000) using a lens detector with an acceleration voltage of 10kV at calibrated magnifications. EM was performed at COMET, MRI facility, Montpellier, France.

Statistics

In order test for differences in the phenotypic distribution of fly populations, we used the two-tailed Fisher’s exact test. To test for differences in eye pigment levels, in RTqPCR experiments, in ChIP signal levels, and FISH distances, we used the two-tailed Student’s *t*-test. To test for differences in relative intensities of Polycomb on FISH signals, we used the two-tailed Mann-Whitney test. In order to compare phenotypes of fly populations in microcosm experiments, linear mixed-model analysis between Week 0 and Week 21 time points was used.

Supplementary Material

Refer to Web version on PubMed Central for supplementary material.

Acknowledgments

This study benefited from the CNRS human and technical resources allocated to the ECOTRONS Research Infrastructure as well as from the state allocation ‘Investissement d’Avenir’ AnaEE-France ANR-11-INBS-0001. We thank J. Roy, S. Devidal, A. Milcu, D. Landais, O. Ravel and A. Faez for help at the Ecotron-CNRS Facility in Montpellier; J. Foucaud, B. Serrate and A. Rombaut for help with conducting experiments on environmental effects in CBGP; J.-M. Chang and V. Loubiere for technical support; M. Siomi (Keio University) for providing the anti-

Aubergine 4D10 antibody; Montpellier Ressources Imagerie facility MRI-IGH for microscopy support. F.C. was supported by the Fondation pour la Recherche Medicale (FRM). F.B. was supported by CNRS. F. Comoglio was supported by ETH Zurich. B.B. was supported by the Sir Henry Wellcome Postdoctoral Fellowship (WT100136MA). Research of R.P. was supported by the FP7 European Network of Excellence EpiGeneSys, the Swiss National Science Foundation and ETH Zurich. M. N. and A. A. were supported by NIH r01 grant GM097363. Research in the laboratory of G.C. was supported by grants from the European Research Council (ERC-2008-AdG No 232947), the CNRS, the FP7 European Network of Excellence EpiGeneSys, the European Union's Horizon 2020 research and innovation programme under grant agreement No 676556 (MuG), the Agence Nationale de la Recherche, the Fondation pour la Recherche Médicale, the INSERM, the French National Cancer Institute (INCa) and the Laboratory of Excellence EpiGenMed.

References

1. Jablonka E, Raz G. Transgenerational Epigenetic Inheritance: prevalence, mechanisms and implications for the study of heredity and evolution. The Quarterly Review Of Biology. 2009; 84
2. Danchin E, et al. Beyond DNA: integrating inclusive inheritance into an extended theory of evolution. Nat Rev Genet. 2011; 12:475–86. [PubMed: 21681209]
3. Heard E, Martienssen RA. Transgenerational epigenetic inheritance: myths and mechanisms. Cell. 2014; 157:95–109. [PubMed: 24679529]
4. Lim JP, Brunet A. Bridging the transgenerational gap with epigenetic memory. Trends Genet. 2013; 29:176–86. [PubMed: 23410786]
5. Daxinger L, Whitelaw E. Understanding transgenerational epigenetic inheritance via the gametes in mammals. Nat Rev Genet. 2012; 13:153–62. [PubMed: 22290458]
6. Houri-Ze'evi L, et al. A Tunable Mechanism Determines the Duration of the Transgenerational Small RNA Inheritance in C. elegans. Cell. 2016; 165:88–99. [PubMed: 27015309]
7. Seong KH, Li D, Shimizu H, Nakamura R, Ishii S. Inheritance of stress-induced, ATF-2-dependent epigenetic change. Cell. 2011; 145:1049–61. [PubMed: 21703449]
8. Dias BG, Ressler KJ. Parental olfactory experience influences behavior and neural structure in subsequent generations. Nat Neurosci. 2014; 17:89–96. [PubMed: 24292232]
9. Zeybel M, et al. Multigenerational epigenetic adaptation of the hepatic wound-healing response. Nat Med. 2012; 18:1369–77. [PubMed: 22941276]
10. Johannes F, et al. Assessing the impact of transgenerational epigenetic variation on complex traits. PLoS Genet. 2009; 5:e1000530. [PubMed: 19557164]
11. Reinders J, et al. Compromised stability of DNA methylation and transposon immobilization in mosaic Arabidopsis epigenomes. Genes Dev. 2009; 23:939–50. [PubMed: 19390088]
12. Greer EL, et al. Transgenerational epigenetic inheritance of longevity in Caenorhabditis elegans. Nature. 2011; 479:365–71. [PubMed: 22012258]
13. Rassoulzadegan M, et al. RNA-mediated non-mendelian inheritance of an epigenetic change in the mouse. Nature. 2006; 441:469–74. [PubMed: 16724059]
14. Xing Y, et al. Evidence for transgenerational transmission of epigenetic tumor susceptibility in Drosophila. PLoS Genet. 2007; 3:1598–606. [PubMed: 17845077]
15. Ashe A, et al. piRNAs can trigger a multigenerational epigenetic memory in the germline of C. elegans. Cell. 2012; 150:88–99. [PubMed: 22738725]
16. Cubas P, Vincent C, Coen E. An epigenetic mutation responsible for natural variation in floral symmetry. Nature. 1999; 401:157–161. [PubMed: 10490023]
17. Manning K, et al. A naturally occurring epigenetic mutation in a gene encoding an SBP-box transcription factor inhibits tomato fruit ripening. Nat Genet. 2006; 38:948–52. [PubMed: 16832354]
18. Morgan HD, Sutherland HG, Martin DI, Whitelaw E. Epigenetic inheritance at the agouti locus in the mouse. Nat Genet. 1999; 23:314–8. [PubMed: 10545949]
19. Kassis JA, Brown JL. Polycomb group response elements in Drosophila and vertebrates. Adv Genet. 2013; 81:83–118. [PubMed: 23419717]
20. Steffen PA, Ringrose L. What are memories made of? How Polycomb and Trithorax proteins mediate epigenetic memory. Nat Rev Mol Cell Biol. 2014; 15:340–56. [PubMed: 24755934]

21. Cavalli G, Paro R. The Drosophila Fab-7 chromosomal element conveys epigenetic inheritance during mitosis and meiosis. Cell. 1998; 93:505–18. [PubMed: 9604927]
22. Dekker J, Mirny L. The 3D Genome as Moderator of Chromosomal Communication. Cell. 2016; 164:1110–21. [PubMed: 26967279]
23. Nguyen HQ, Bosco G. Gene Positioning Effects on Expression in Eukaryotes. Annu Rev Genet. 2015; 49:627–46. [PubMed: 26436457]
24. Dixon JR, Gorkin DU, Ren B. Chromatin Domains: The Unit of Chromosome Organization. Mol Cell. 2016; 62:668–80. [PubMed: 27259200]
25. Ciabrelli F, Cavalli G. Chromatin-driven behavior of topologically associating domains. J Mol Biol. 2015; 427:608–25. [PubMed: 25280896]
26. Bantignies F, Grimaud C, Lavrov S, Gabut M, Cavalli G. Inheritance of Polycomb-dependent chromosomal interactions in Drosophila. Genes Dev. 2003; 17:2406–20. [PubMed: 14522946]
27. Zink D, Paro R. Drosophila Polycomb-group regulated chromatin inhibits the accessibility of a trans-activator to its target DNA. Embo J. 1995; 14:5660–71. [PubMed: 8521823]
28. Kyrchanova O, et al. Functional Dissection of the Blocking and Bypass Activities of the Fab-8 Boundary in the Drosophila Bithorax Complex. PLoS Genet. 2016; 12:e1006188. [PubMed: 27428541]
29. Bantignies F, et al. Polycomb-Dependent Regulatory Contacts between Distant Hox Loci in Drosophila. Cell. 2011; 144:214–26. [PubMed: 21241892]
30. Li HB, et al. Insulators, not Polycomb response elements, are required for long-range interactions between Polycomb targets in Drosophila melanogaster. Mol Cell Biol. 2011; 31:616–25. [PubMed: 21135119]
31. Li HB, Ohno K, Gui H, Pirrotta V. Insulators target active genes to transcription factories and polycomb-repressed genes to polycomb bodies. PLoS Genet. 2013; 9:e1003436. [PubMed: 23637616]
32. Sievers C, Comoglio F, Seimiya M, Merdes G, Paro R. A deterministic analysis of genome integrity during neoplastic growth in Drosophila. PLoS One. 2014; 9:e87090. [PubMed: 24516544]
33. Hodgetts R, Choi A. Beta alanine and cuticle maturation in Drosophila. Nature. 1974; 252:710–1. [PubMed: 4215980]
34. Pilu R. Paramutation: just a curiosity or fine tuning of gene expression in the next generation? Curr Genomics. 2011; 12:298–306. [PubMed: 22131875]
35. de Vanssay A, et al. Paramutation in Drosophila linked to emergence of a piRNA-producing locus. Nature. 2012; 490:112–5. [PubMed: 22922650]
36. Tolhuis B, et al. Interactions among Polycomb Domains Are Guided by Chromosome Architecture. PLoS Genet. 2011; 7:e1001343. [PubMed: 21455484]
37. Mahmoudi T, Katsani KR, Verrijzer CP. GAGA can mediate enhancer function in trans by linking two separate DNA molecules. Embo J. 2002; 21:1775–1781. [PubMed: 11927561]
38. Dejardin J, et al. Recruitment of Drosophila Polycomb group proteins to chromatin by DSP1. Nature. 2005; 434:533–8. [PubMed: 15791260]
39. Schuettengruber B, et al. Functional Anatomy of Polycomb and Trithorax Chromatin Landscapes in Drosophila Embryos. PLoS Biol. 2009; 7:e13. [PubMed: 19143474]
40. Iovino N, Ciabrelli F, Cavalli G. PRC2 controls Drosophila oocyte cell fate by repressing cell cycle genes. Dev Cell. 2013; 26:431–9. [PubMed: 23932903]
41. Herzog VA, et al. A strand-specific switch in noncoding transcription switches the function of a Polycomb/Trithorax response element. Nat Genet. 2014; 46:973–81. [PubMed: 25108384]
42. Pirrotta V, Rastelli L. White gene expression, repressive chromatin domains and homeotic gene regulation in Drosophila. Bioessays. 1994; 16:549–56. [PubMed: 7916186]
43. Lynch, M., Walsh, B. Genetics and Analysis of Quantitative Traits. Sinauer; 1998.
44. Talbert PB, Garber RL. The Drosophila homeotic mutation Nasobemia (AntpNs) and its revertants: an analysis of mutational reversion. Genetics. 1994; 138:709–20. [PubMed: 7851768]

45. Melnikova L, et al. Interaction between the GAGA factor and Mod(mdg4) proteins promotes insulator bypass in Drosophila. Proc Natl Acad Sci U S A. 2004; 101:14806–11. [PubMed: 15465920]

46. Bantignies F, Cavalli G. Topological organization of Drosophila hox genes using DNA fluorescent in situ hybridization. Methods Mol Biol. 2014; 1196:103–20. [PubMed: 25151160]

47. Langmead B, Salzberg SL. Fast gapped-read alignment with Bowtie 2. Nat Methods. 2012; 9:357–9. [PubMed: 22388286]

48. Li H, et al. The Sequence Alignment/Map format and SAMtools. Bioinformatics. 2009; 25:2078–9. [PubMed: 19505943]

49. Obenchain V, et al. VariantAnnotation: a Bioconductor package for exploration and annotation of genetic variants. Bioinformatics. 2014; 30:2076–8. [PubMed: 24681907]

50. Eden E, Navon R, Steinfeld I, Lipson D, Yakhini Z. GOrilla: a tool for discovery and visualization of enriched GO terms in ranked gene lists. BMC Bioinformatics. 2009; 10:48. [PubMed: 19192299]

51. Thorvaldsdottir H, Robinson JT, Mesirov JP. Integrative Genomics Viewer (IGV): high-performance genomics data visualization and exploration. Brief Bioinform. 2013; 14:178–92. [PubMed: 22517427]

52. Langmead B, Trapnell C, Pop M, Salzberg SL. Ultrafast and memory-efficient alignment of short DNA sequences to the human genome. Genome Biol. 2009; 10:R25. [PubMed: 19261174]

53. Quinlan AR, Hall IM. BEDTools: a flexible suite of utilities for comparing genomic features. Bioinformatics. 2010; 26:841–2. [PubMed: 20110278]

54. Love MI, Huber W, Anders S. Moderated estimation of fold change and dispersion for RNA-seq data with DESeq2. Genome Biol. 2014; 15:550. [PubMed: 25516281]

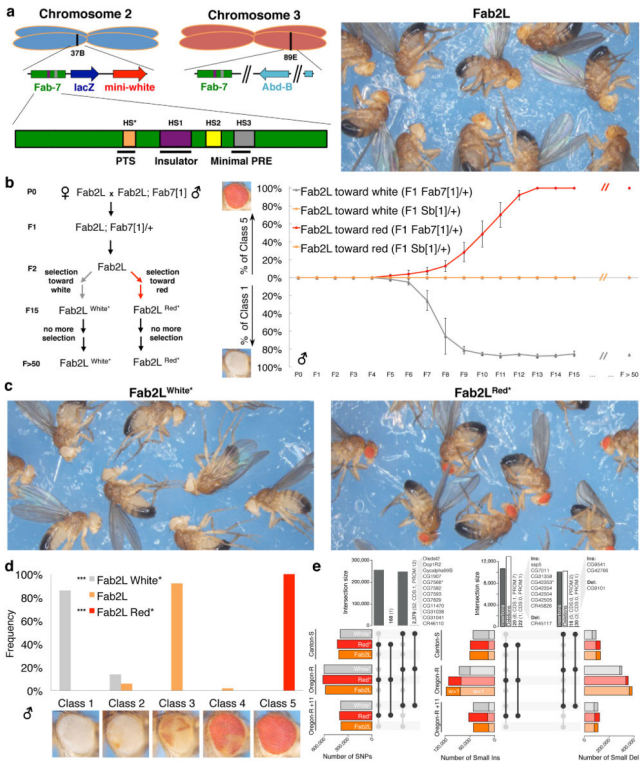

Figure 1.

Establishment of stable *Drosophila* epilines via transient genetic perturbation. (**a**) Illustration of Fab2L transgene insertion site in cytological position 37B and of the endogenous *Fab-7* in cytological position 89E. The boxes within the *Fab-7* region represent DNAse I hypersensitive sites (HS), partially overlapping with some functional elements. The right picture shows a representative sample of Fab2L males reared at 21°C. (**b**) Crossing scheme for the establishment of the epilines. On the right, the curves represent the percentages of Class 1 (white-eyed) and Class 5 (red-eyed) male flies at each generation. The phenotypic trends of control Fab2L; +/+ flies (*Sb[1]/+* in F1) are represented in orange. The phenotypic trends of Fab2L; +/+ flies (*Fab7[1]/+* F1), selected for more or less pigment, are represented in red and grey, respectively. At each generation, 6 to 12 flies of each sex were selected on a total progeny of 120>n>40 flies (n>150 for each sex in F2). Points represent the mean +/− s. d. of n=3 independent crosses. (**c**) Pictures showing a representative sample of Fab2L^{White*} and Fab2L^{Red*} males reared at 21°C. (**d**) Phenotypic classification based on eye pigment levels in Fab2L^{White*} (n=200), Fab2L (n=218) and Fab2L^{Red*} (n=229) male flies. Class 1: pigment=0%; Class 2: 0%<pigment≤5%; Class 3: 5%<pigment≤75%; Class 4: 75%<pigment<100%; Class 5: pigment=100%. (**e**) On the left, total number of identified SNPs and intersection between epilines. Putative phenotype-associated SNPs are those exclusively identified in a given epiline in both genetic backgrounds and across generations (second and fourth vertical bar, respectively). The total number of homozygous events is indicated in brackets. Events occurring within coding sequences (CDS) or promoters (PROM) are further detailed. On the right, same as left panel, but for the identified small insertions (Ins) and deletions (Del). w, weight, i.e. the number of discordant read pairs

supporting a given structural variation. Bars represent the frequency (**d**) or the number of events (**e**); two-tailed Fisher's exact test. NS $P>0.05$; * $P<0.05$; ** $P<0.01$; *** $P<0.001$.

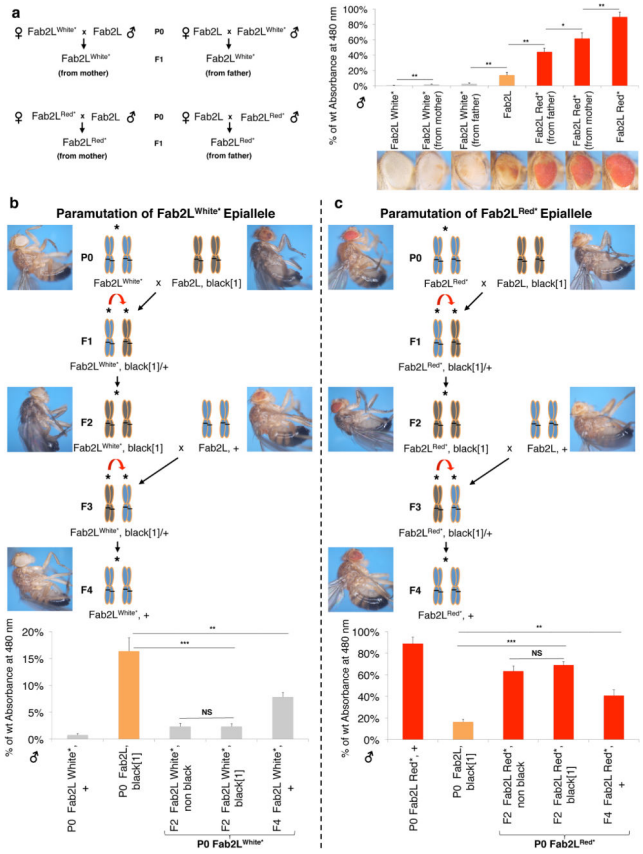

Figure 2.

Epiallele inheritance displays pseudodominance, parent-of-origin effect, and paramutagenicity. (**a**) Crossing schemes, eye pigmentation assays and representative pictures of the observed phenotypes in the dominance tests. (**b**,**c**) Crossing schemes, representative pictures of the observed phenotypes and eye pigmentation assays of the paramutation tests. The blue chromosomes represent chromosome 2, the grey chromosomes represent chromosome 2 carrying the *black[1]* allele, the black lines represent the transgenic insertion, the asterisks indicate the presence of the epiallele and the curved red lines indicate the paramutation events. The pictures display the representative body-color and eye-color phenotypes observed in the P0, F2 and F4 generations. F2 “non black” indicates flies with a wild type body color phenotype, having either a +/+ or a +/black[1] genotype. Bars represent the mean of n=3 independent crosses +/− s. d.; two-tailed Student’s *t*-test: NS $P>0.05$; * $P<0.05$; ** $P<0.01$; *** $P<0.001$.

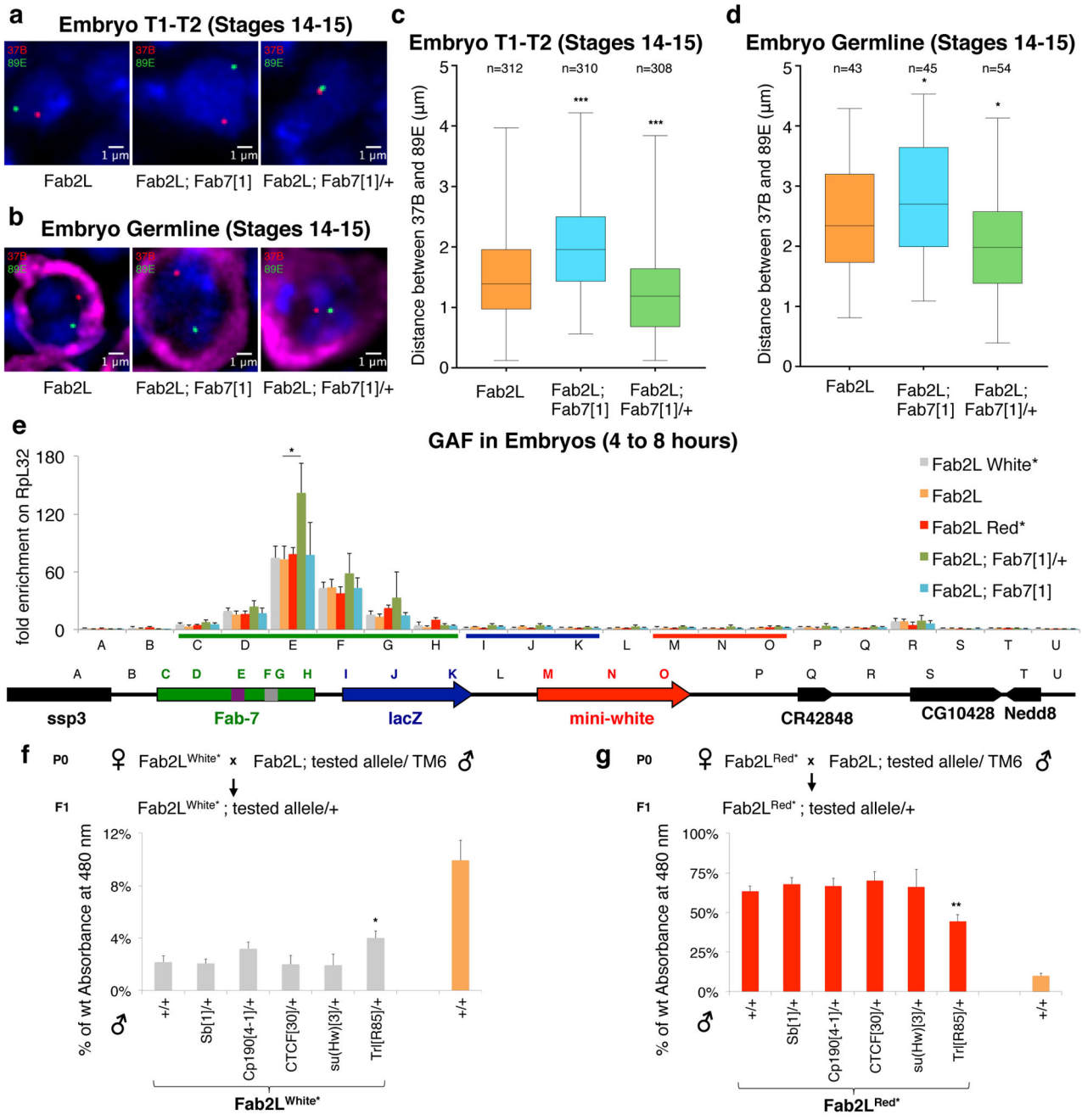

Figure 3.

Enhanced long-range chromatin interactions underlie epiallele establishment. (**a**,**b**) Representative pictures of the FISH-I assays performed in the indicated genotypes. Nuclei are stained with DAPI in blue, *37B* locus is stained in red and *89E* locus is stained in green. The cytoplasm of germline nuclei is stained in magenta with anti-Aubergine. Scale bar is 1 µm. (**c**,**d**,) Box plots representing the distance distributions of the FISH-I assays performed in the indicated genotypes between the *37B* and the *89E* loci. Distances are measured in stage 14–15 embryos in T1 and T2 segments or in the germline. The centerline represents the median, the box delimits the interquartile-range and the limits define the distribution

range. In the figure, n represents the total number of nuclei analyzed from 3 embryos. (**e)** ChIP-qPCR assays performed in the indicated genotypes in 4 to 8 hours embryos, showing relative enrichments (ChIP/Input) for GAF, normalized to a negative control. Amplicon locations are indicated below the charts. (**f,g**) Crossing schemes and eye pigmentation assays performed on Fab2L (orange), Fab2L^{White*} (grey) and Fab2L^{Red*} (red) male flies, combined with the tested alleles on chromosome 3. Bars represent the mean of n=3 independent embryo collections (**e**) or independent crosses (**f-g**) +/− s. d. (**e-g**); two-tailed Student's *t*-test: NS $P>0.05$; * $P<0.05$; ** $P<0.01$; *** $P<0.001$.

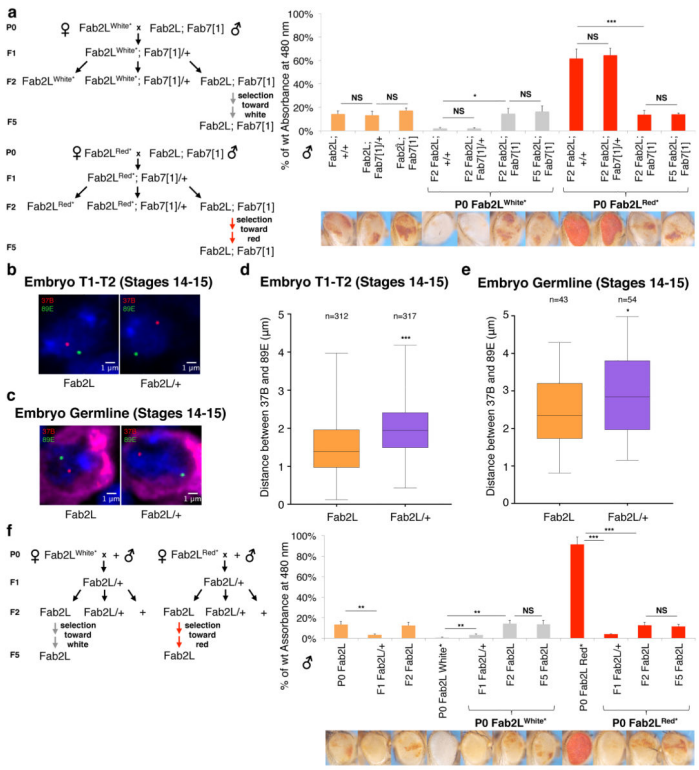

Figure 4.

Long-range chromatin interactions are necessary for epiallele maintenance. (**a,f**) Crossing schemes, eye pigmentation assays and representative pictures of the observed phenotypes in the epiallele maintenance tests. (**b,c**) Representative pictures of the FISH-I assays performed in the indicated genotypes. Nuclei are stained with DAPI in blue, *37B* locus is stained in red and *89E* locus is stained in green. The cytoplasm of germline nuclei is stained in magenta with anti-Aubergine. Scale bar is 1 µm. (**d,e**) Box plots representing the distance distributions of the FISH-I assays performed in the indicated genotypes between the *37B* and the *89E* loci. Distances are measured in stage 14–15 embryos in T1 and T2 segments or in the germline. The centerline represents the median, the box delimits the interquartile-range and the limits define the distribution range. In the figure, n represents the total number of nuclei analyzed from 3 embryos. Bars represent the mean of n=3 independent crosses +/− s. d. (**a,f**); two-tailed Student's *t*-test: NS $P>0.05$; * $P<0.05$; ** $P<0.01$; *** $P<0.001$.

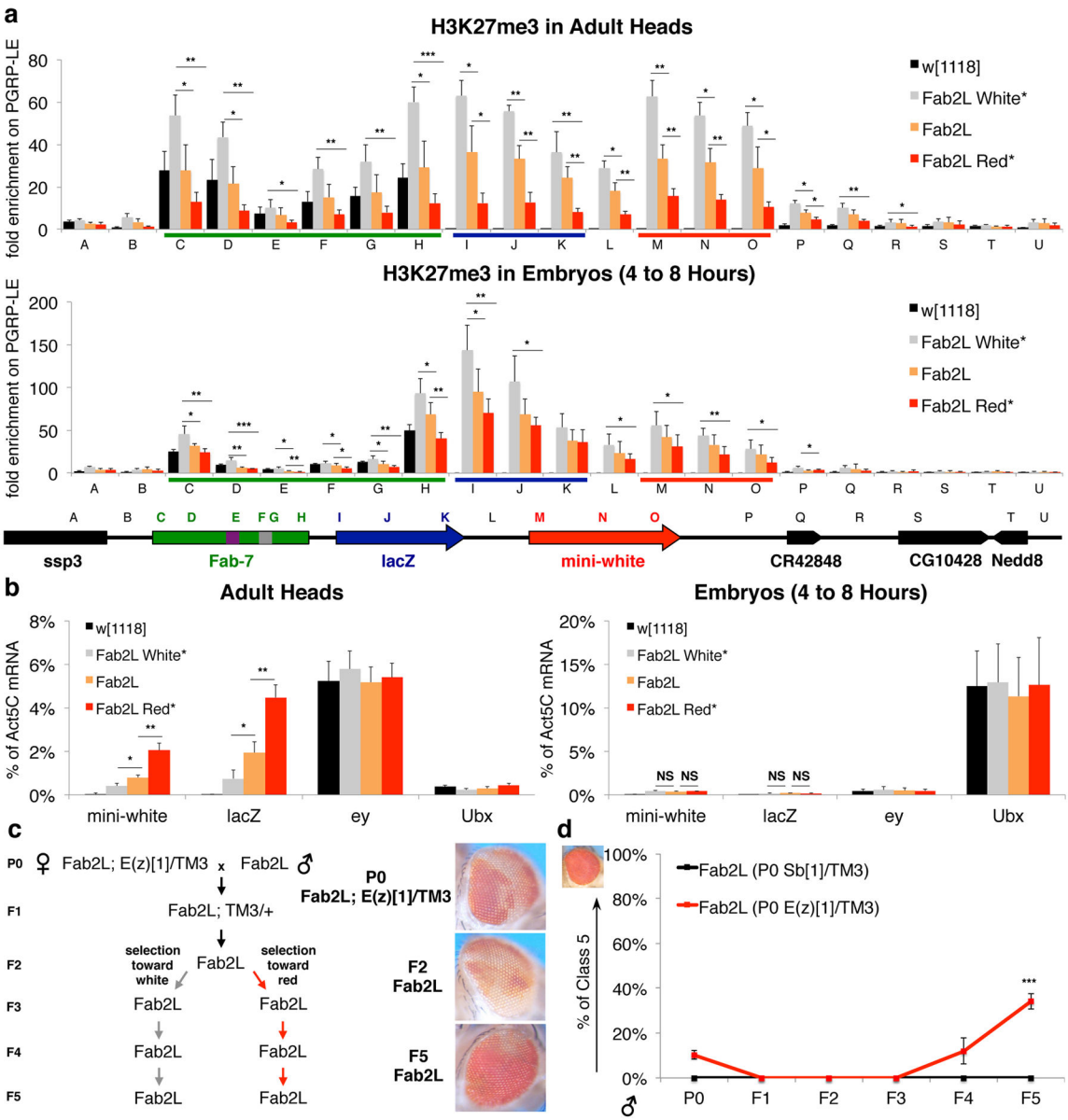

Figure 5.

PRC2 activity determines alternative chromatin states of the epialleles. (**a**) ChIP-qPCR assays performed on w[1118], Fab2L^{White*}, Fab2L and Fab2L^{Red*} male adult heads and 4 to 8 hours embryos, showing relative enrichments (ChIP/Input) for H3K27me3, normalized to a negative control. Amplicon locations are indicated below the charts. (**b**) RT-qPCR assays performed on w[1118], Fab2L^{White*}, Fab2L and Fab2L^{Red*} male adult heads, and 4 to 8 hours embryos, measuring relative mRNA levels normalized to *Act5C.* (**c**) Crossing schemes and representative pictures of the observed phenotypes in the P0, F2 and F5 in the epiallele establishment test. (**d**) Curves in the chart representing the percentage of Class 5 (pigment=100%) male flies at each generation during the phenotypic selection. The phenotypic trend of Fab2L; +/+ flies that had the control *Sb[1]* allele during the P0, selected for more pigment, is represented in black. The phenotypic trend of Fab2L; +/+ flies that had

the *E(z)[1]* allele in the P0, selected for more pigment, is represented in red. At each generation, 6 to 8 flies for each sex were selected on a total progeny of 30>n>60 individuals. Bars represent the mean +/− s. d. of n=3 independent collections of adult heads for ChIP or RT-qPCR (**a,b**), or embryos for RT-qPCR (**b**); n=4 for embryo ChIP (**a**); Error bars in panel **d** represent s. d. of n=3 independent crosses; two-tailed Student's *t*-test: NS $P>0.05$; * $P<0.05$; ** $P<0.01$; *** $P<0.001$.

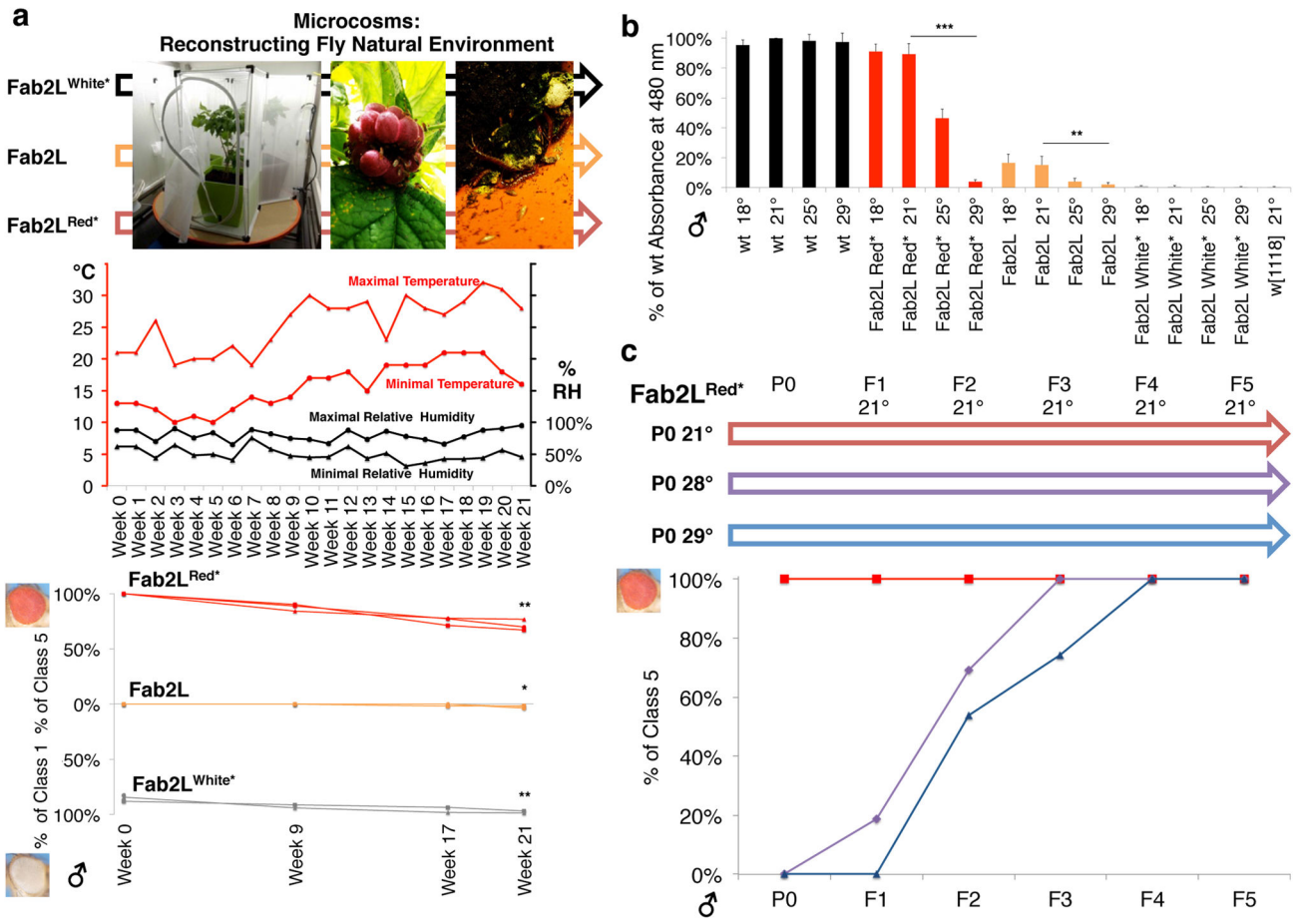

Figure 6.

Environmental effects on the epialleles. (**a**) Schematic representation and illustrative pictures of epiline exposure to natural conditions. The top chart shows maximal and minimal temperature and relative humidity in the reproduced weeks. The bottom chart represent the percentage of Class 1 (pigment=0%) and percentage of Class 5 (pigment=100%) flies at 4 time points; n=3 independent fly populations exposed; linear mixed-model analysis between Week 0 and Week 21 time points: NS $P>0.05$; * $P<0.05$; ** $P<0.01$; *** $P<0.001$. (**b**) Eye pigmentation assays performed on wt, Fab2L^{Red*}, Fab2L, Fab2L^{White*} and w[1118] male and flies after at least two-generation exposure to the indicated temperatures. Bars represent the mean of n=3 independent fly collections +/− s. d.; two-tailed Student's *t*-test: NS $P>0.05$; * $P<0.05$; ** $P<0.01$; *** $P<0.001$. (**c**) Self-crossing scheme performed at 21°C, starting from Fab2L^{Red*} flies previously reared at 21°C, 28°C or 29°C. Phenotypic classification of the eye pigment levels. The curves in the chart represent the percentage of Class 5 (pigment=100%) male flies at each generation. At each point n>30 male flies were scored.

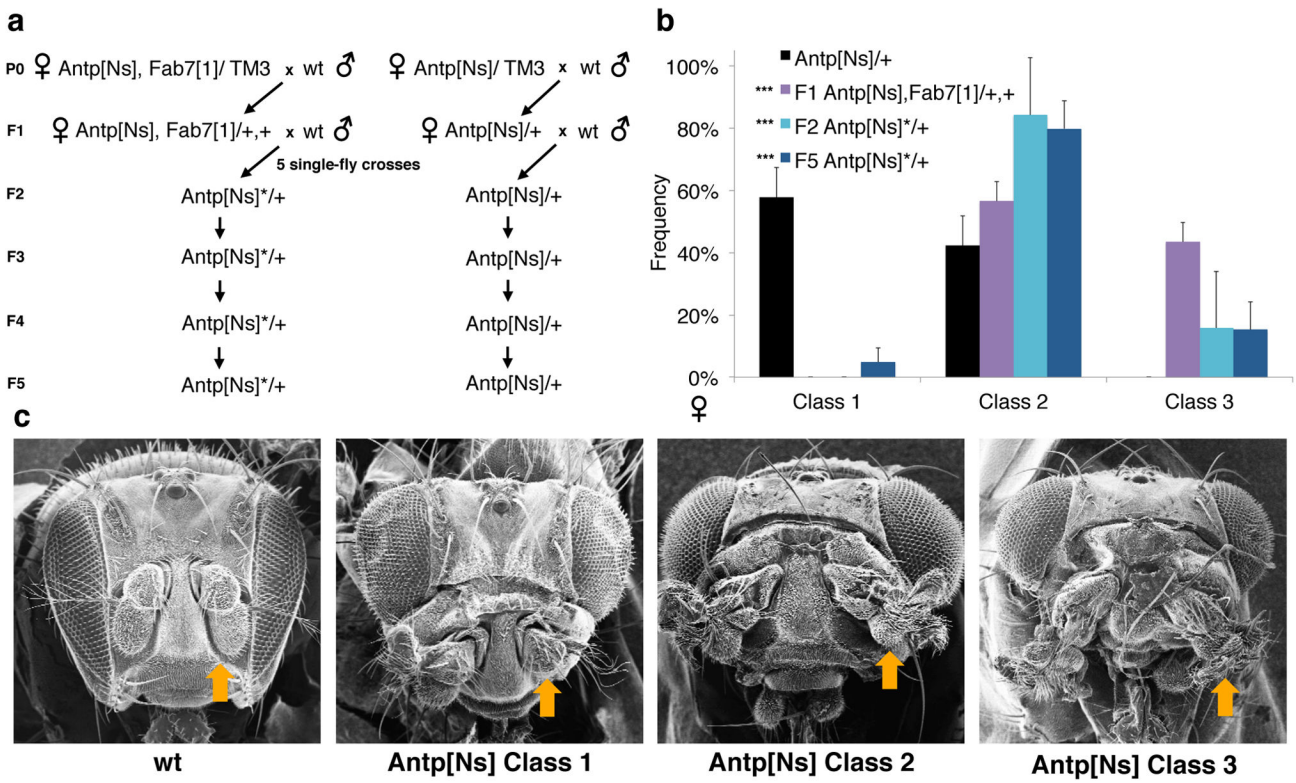

Figure 7.

TEI of a homeotic trait. (**a**) Crossing schemes and (**b**) charts representing the phenotypic distributions of the Antp[Ns] homeotic transformation phenotype in adult females for each generation. (**c**) Representative pictures, showing phenotypic distribution of the Antp[Ns] homeotic transformation phenotype. The yellow arrows in the pictures indicate the transformation phenotypes. Phenotypic classification of the antenna to leg transformation phenotype. Class 1: weak transformation; Class 2: medium transformation; Class 3: severe transformation. Bars represent the mean of the frequencies of n=5 parallel single-fly crosses, deriving from independent recombination events in the F1, +/− s. d.; two-tailed Fisher's exact test: NS $P>0.05$; * $P<0.05$; ** $P<0.01$; *** $P<0.001$. Fisher's exact test was applied on the pooled populations from the 5 independent single-fly crosses at each generation. After pooling, flies were n>50 for each genotype.

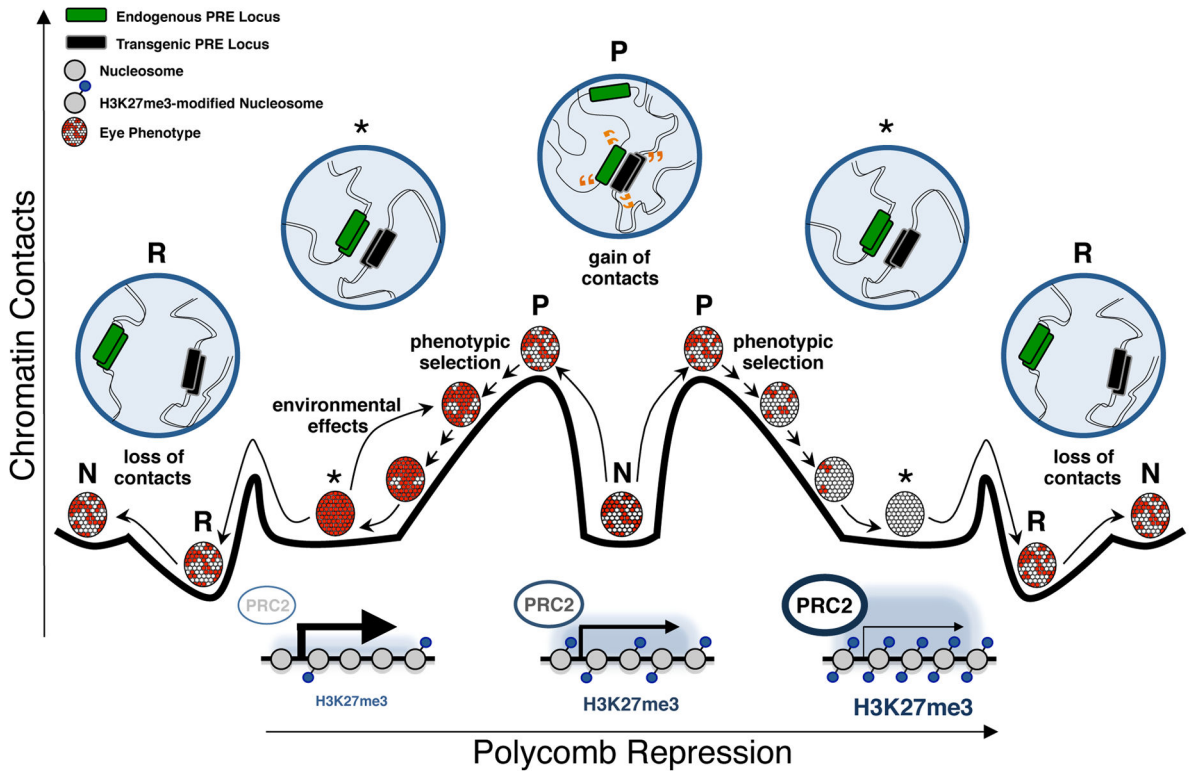

Figure 8.

Epiallele induction by long-range chromatin interactions and differential H3K27me3 marking. In this schematic representation, summarizing epiallele establishment and reversion, the variegated eye represents the naïve "**N**" epigenetic state of Fab2L flies. After a gain in chromatin contacts between the endogenous locus and the transgenic locus, the latter acquires a primed "**P**" epigenetic state. The primed "**P**" epigenetic state has the potential to reach a stable " * " epigenetic state, upon phenotypic selection. The stable " * " epigenetic state can be modulated by environmental factors, and it can be stably reverted by a loss of chromatin contacts, into a "**R**" epigenetic state. The bottom pictures represent the corresponding chromatin states of the naïve flies and the epilines. They show increasing enrichments for the H3K27me3 mark and an opposite trend for their transcriptional states.